MEDWIN PUBLISHERS
Committed to create value for Researchers

Physical Science & Biophysics Journal
ISSN: 2641-9165

Assessing the Chemical Activity of Plasma Radiation

Aristova NA[1] and Piskarev IM[2]*

[1]Nizhny Tagil Technological Institute, Ural Federal University Branch, Russia

[2]Skobeltsyn Institute of Nuclear Physics, 119234, Leninskie Gory, Moscow, Russia

***Corresponding author**: Skobeltsyn Institute of Nuclear Physics, 119234, Leninskie Gory, MSU, 1 (2), Moscow, Russian Federation, E-mail: i.m.piskarev@gmail.com

Research Article

Volume 3 Issue 2

Received Date: June 06, 2019

Published Date: June 26, 2019

Abstract

The chemical activity of products formed under the action of spark discharge plasma radiation in aqueous solutions was investigated. The red-ox reactions with the test substances were used to determine of chemical effect of plasma radiation. Aqueous solutions of Mohr's salt and potassium permanganate were used as test substances. Two cases of irradiation were studied: directly on the test substance solution (case 1) and on water, after which the treated water was mixed with the test substance (case 2). The yield of oxidizing equivalents formed in the sample during treatment was determined for the both cases by oxidation of ferrous ions $Fe^{2+} \rightarrow Fe^{3+}$ in the Mohr's salt solution. The yield of reducing equivalents was determined by reduction of manganese $Mn^{7+} \rightarrow Mn^{2+}$ in solution of potassium permanganate. Three processing modes were used. Mode 1, the direction from the discharge area to the surface of treated liquid has been opened. Mode 2, the direction from the discharge area to the surface of treated liquid was blocked by an opaque plate. Mode 3, the discharge cavity was completely closed by a 2.3 mm thick quartz glass. For comparison, the yield of oxidizing and reducing equivalents under the action of mercury lamp radiation (λ = 253.7 nm) was measured. For the complete yield of reductants and oxidizing agents, the yield of suitable reactions was taken on the 4^{th} day after treatment. It was shown that the main mechanism of the reaction under plasma radiation is indirect action.

Keywords: Plasma radiation; Yield of oxidation; Yield of reduction; Indirect action of radiation; Delay of reaction

Introduction

Cold plasma can come into direct contact with an object without causing thermal damage. As such, cold plasma treatment is used to act on the chemical composition of water and aqueous solutions [1,2]. The peculiarity of this treatment type is that the concentration of active species in plasma is high, so there is a high probability of termination due to the interaction of these species [3]. Because of this effect, there is a decrease in efficiency of plasma treatment.

Spark discharge plasma radiation also produces a strong chemical effect in a liquid sample [4]. The plasma that generates the radiation is created from a spark discharge between the electrodes at a considerable

distance from the sample. There is no gas flow from the discharge area to the sample, so the products formed in the electric discharge plasma do not directly interact with the processed liquid. Relatively long-lived gaseous products formed in the discharge can diffuse to the surface of the liquid and be absorbed. These products also create a chemical effect.

Past research has considered the composition and characteristics of products formed under the radiation of spark electric discharge between solid electrodes, as well as products diffused from the discharge region [5,6]. These products initiate a redox reaction in an aqueous solution. It is interesting to study the characteristics of these reactions.

The goal of the work is to study the chemical activity of plasma radiation and related products of spark discharged into air. This goal is achieved using redox reactions in aqueous solutions.

Materials and Methods

One source of spark discharge plasma radiation was the generator SD50 [5]. The experimental set-up is shown in Figure 1. The spark discharge occurred between the solid electrodes connected to the discharge capacitor, C_D = 680 pF. A high voltage of 11 kV was applied to the capacitor via the ballast resistance, R_D = 8 MOhm. The self-supporting spark discharge began when the high voltage was turned on. The pulse duration of the full current was 5 μs, with a front of 50 ns, a pulse energy of 8.1 x 10^{-3} J, a pulse repetition frequency 50 Hz and the power of the discharge was 0.4 J/s. The duration of the current pulse was determined by the dissipation time of the charge in spark channel. The current consumed from the power supply was 0.7 ± 0.02 mA. Previous work considered the characteristics of the spark discharge plasma that is used in this work [5]. The outlet from the discharge cavity had a diameter of 20 mm, the distance from the discharge area to the surface of the treated liquid was 30 mm. The light spot on the surface of the sample had a diameter of 40 mm. Samples were processed in Petri dishes with diameters of 40 mm (volume of 5 mL, surface of 12.5 cm^2 and liquid layer thickness of 4 mm) (Figure 1a) and 70 mm (volume of 50 mL, surface of 38.5 cm^2 and liquid layer thickness of 13 mm) (Figure 1b), respectively. Therefore, a 5 mL dish was completely submerged into plasma radiation field; a 50 mL irradiated dish was only exposed to part of the surface, while the rest of the surface was in contact only with gaseous products.

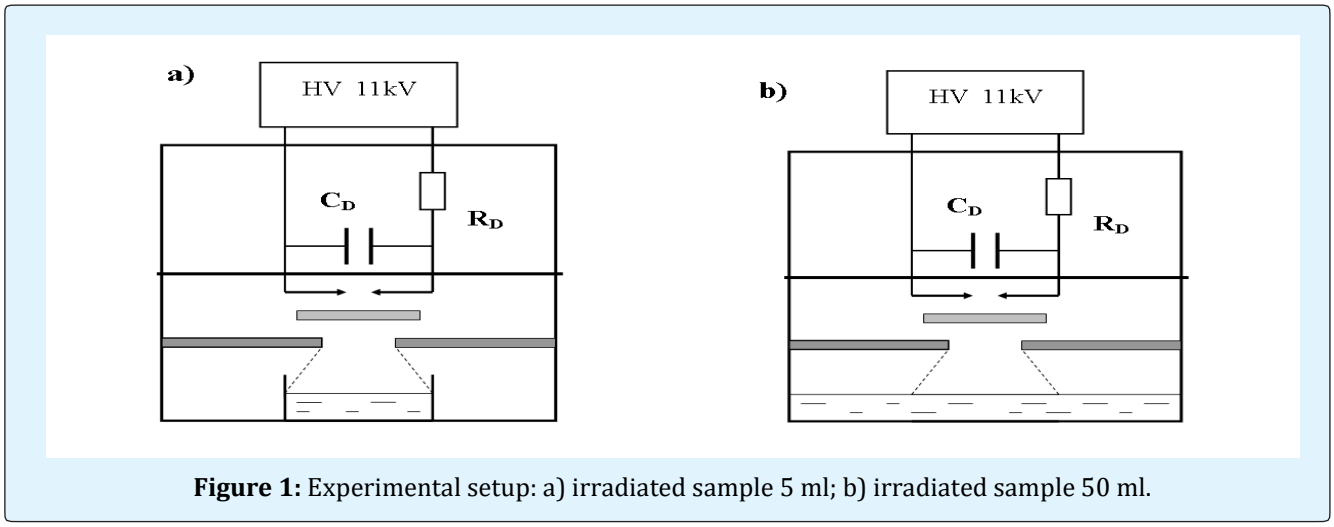

Figure 1: Experimental setup: a) irradiated sample 5 ml; b) irradiated sample 50 ml.

Three processing modes were used. Mode "All" was used when the direction from the discharge area to the liquid surface was opened. In this mode, both plasma radiation and products formed in the discharge acted on the water. The “Gas” Mode was used when the direction to the discharge area was blocked by an opaque plate; the installation of plate is shown in Figure 1. The products formed in the discharge itself could bend around the plate and diffuse to the water surface. The "Quartz" Mode was used when the discharge cavity was closed by a 2.3 mm thick quartz glass. The passage of gaseous products from the discharge cavity to the treated sample was completely excluded. The absorbance for quartz glass is presented in Figure 2.

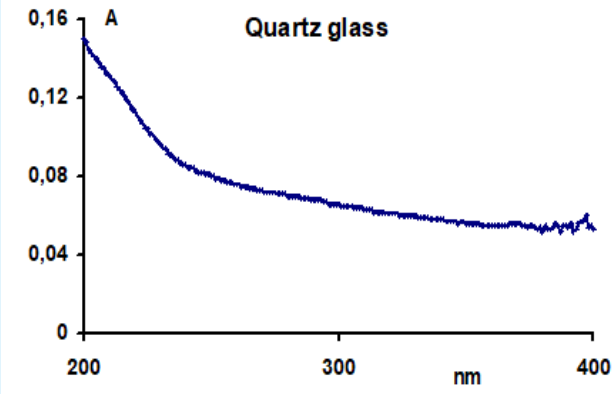

Figure 2: Absorbance of quartz glass 2.3 mm thickness, used in experiment.

Conducting the plasma radiation identified the formation of $HO_2^{\bullet}$ radicals, hydrogen peroxide, nitrous acid decaying into nitric acid and complexes, which were not directly observed and decayed for up to 14 days to peroxynitrite and peroxynitrous acid [5,7]. Hydroxyl radicals are not formed in water under the action of plasma radiation [7]. Radicals formed in discharge itself terminate in discharge region and cannot diffuse to the surface of the sample. Only relatively long-lived nitrogen oxides can diffuse to the sample.

The source of continuous radiation was a low-pressure mercury lamp DKB-9, with a radiation wavelength, λ, of 253.7 and a lamp power of 9 J/s. The lamp body was made of ultraviolet glass, which prevented radiation with a wavelength less than 200 nm from escaping. To ensure stable operation, the lamp was heated for two hours prior to the measurement. The distance from the lamp surface to the sample was 30 mm. When irradiated with a mercury lamp, the entire surface of the sample was exposed.

To determine the chemical effect of radiation, redox reactions with the test substances were used. Aqueous solutions of Mohr's salt and potassium permanganate were used as test substances. Two cases of irradiation were used: (1) directly on the test substance solution, and (2) on water, after which the treated water was mixed with the test substance. The yield of oxidizing equivalents formed in the sample during the treatment was determined for both cases by oxidation of ferrous iron, Fe^{2+} to Fe^{3+} in the Mohr's salt solution. The yield of reducing equivalents was determined by the reduction of manganese from Mn^{7+} to Mn^{2+} in a potassium permanganate solution.

The concentration of Mohr's salt was 20 g/L, $[Fe^{2+}]$ = 5.1 x 10^{-2} mol/L for case 1, and 2 g/L, $[Fe^{2+}]$ = 5.1 10^{-3} mol/L for case 2. Then, 21 ml/L of concentrated sulfuric acid (0.4M) were added to the solution. The solution had a pH of 0.8. The Fe^{2+} concentration in the sample in all experiments was chosen so that the ferrous iron was not completely oxidized. The concentration of oxidized Fe^{3+} was determined by absorbance at 304 nm, where ε = 2100 ± 50 L(mol cm)$^{-1}$. The extinction coefficient was determined directly from the calibrated solution. The background change in the absorbance of this line in initial solution during 4 days (time to measure absorbance of treated sample) was considered. If the absorbance of the sample after treatment exceeded 2, sample was diluted with 0.4M sulfuric acid.

The concentration of potassium permanganate used in the treatment was 1.58 g/L (0.05N). To the solution 21 mL/L of sulfuric acid (0.4M) was added. To observe the absorption peaks in the region 400 – 650 nm, the initial and treated solutions were diluted with water 10 times. The concentration of potassium permanganate was determined by the absorbance of line 527 nm. The extinction coefficient of 527 nm line, measured directly for the calibrated solution, was ε = 2160 ± 50 L(mol cm)$^{-1}$.

The absorption spectra of the samples were measured by a spectrophotometer SF-102 (Akvilon Firm, Russia). The thickness of the cuvette is 10 m. The absorbance $A = \lg(I_0/I)$ Bel was determined relative to distilled water. The pH value was measured by the device Expert-001 (Ekonics Firm, Russia). Distilled water pH = 5.8 and chemically pure reagents were used.

Experimental Results

Changes in the Acidity of Water Sample

After processing the water sample with the spark discharge generator SD50, the pH value decreased and the water became chemically active. The results of pH measurements of the 5 mL water sample after treatment in different modes are presented in Figure 3. That figure also provides pH values after exposure to the mercury lamp (UV). When subjected to UV radiation of the lamp (λ = 253.7 nm), the pH values within the experimental errors do not change. After exposure to generator SD50, the pH values continually decreased. It decreased and after treatment only with UV radiation of spark discharge,

when the light passed through the quartz glass. This result implies that majority of the chemical activity of water is achieved by radiation when wavelength was less than 250 nm. Without quartz glass, the pH decreased faster and reached lower values. This rapid decrease may be due to the absorption of light in quartz glass. In both "All" and "Gas" modes, the pH values are approximately the same.

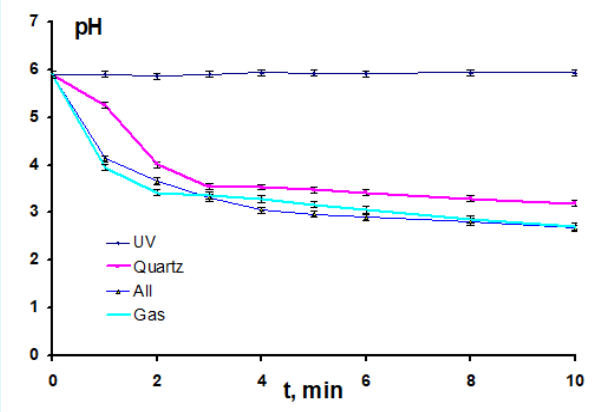

Figure 3: Value of pH water sample 5 mL after irradiated by mercury lamp (UV) and generator SD50 in various modes: Quartz, All and Gas. Time t–minutes.

Oxidation of Ferrous Iron by Products Formed Under the Action of Plasma Radiation

The Time of Oxidation of Divalent Iron in Mohr's Salt: Under plasma radiation, the formation of $HO_2^{\bullet}$ radicals, hydrogen peroxide and nitrogen compounds (nitrous acid and long-lived complex) were identified [5,7]. Nitrogen compounds are also formed in the sample after the absorption by water of products diffused from the discharge region. For different oxidants, there are different rate constants of the reactions with ferrous iron. A portion of oxidizing agents interacts slowly which in turn determines the total reaction time. The decay of long-lived complex can also contribute to the yield of redox reaction, as long as this contribution is greater than the measurement error. Therefore, to determine the concentration of the formed species, each reaction with every oxidant formed under specific processing conditions was considered separately and the time required to complete each reaction was determined. In this case, the post-effects in the treated liquid is not considered, since if the experiments were conducted in the absence of reagents, for pure water, the life time of produced species could be much longer [6].

Reactions under UV Radiation and with Hydrogen Peroxide: A low pressure mercury lamp was used to estimate the reaction time under a UV radiation of 253.7 nm. The Mohr's salt solution with concentration of 2 g/L and a volume of 5 ml was treated with a UV lamp radiation for 10 minutes. Immediately after treatment, the absorbance (A) was 0.86 ± 0.05. This value does not change for four days. To estimate the reaction time with hydrogen peroxide, 0.1 ml of 0.03% H_2O_2 was introduced into the 5 ml Mohr's salt solution of the same concentration. Immediately after mixing, A = 0.75 ± 0.05. Over the next four days, this value also does not change.

Bivalent iron does not directly absorb a photon when λ = 253.7 nm; therefore, reactions under the action of UV radiation of mercury lamp occur through the formation of hydrogen peroxide [8].

$$H_2O + h\nu \rightarrow H_2O \quad (1)$$

$$H_2O^{\bullet} + H_2O \rightarrow H_2O_2 + H_2 \quad (2)$$

Here, reaction 2 can go through the stage of immediate products generation: radicals $HO_2^{\bullet}$, the interaction of which one another leads to the formation of hydrogen peroxide. The yield of $HO_2^{\bullet}$ radicals was previously estimated [7]. Furthermore, the hydrogen peroxide oxidizes ferrous iron.

$$H_2O_2 + Fe^{2+} \rightarrow Fe^{3+} + OH^{\bullet} + OH^{-} \quad (3)$$

Reaction 3 is relatively slow (k_3 = 56 L(mol s)$^{-1}$) [9]. The reaction time here is tens of seconds and continues until the complete consumption of hydrogen peroxide. According to the obtained experimental data, this reaction ends in about 1.5 minutes, which is necessary to install the sample after UV irradiation in a spectrophotometer. From this result, the reaction under the UV radiation and hydrogen peroxide is fairly quick, as it does not last longer than 1.5 minutes.

Reactions with Nitrous Acid and Products Formed under the Action of Spark Discharge Radiation: First, 0.1 ml of an aqueous solution of $NaNO_2$ (concentration of 0.1 mol/L) was added to 5 ml of a 2 g/L Mohr's salt solution. The mixture was immediately diluted 10 times with 0.4 M sulfuric acid. In this case sodium nitrite was transformed into nitrous acid.

$$2NaNO_2 + H_2SO_4 \rightarrow 2HNO_2 + Na_2SO_4 \quad (4)$$

In the sample, ferrous iron was oxidized with nitrous acid. Immediately after the introduction of $NaNO_2$, the absorbance of the 304 nm line, attributable to Fe^{3+}, is

small. This absorbance increases with time until it reaches a plateau. The value of the absorbance on the plateau is defined as Ap, and the value of absorbance at a given time is defined as At. The dependence of the ratio Ap/At over time after the introduction of $NaNO_2$ to a Mohr's salt solution is presented in Figure 4**.** The reaction with nitrous acid is slow and lasts up to two days (Figure 4, curve 1). This result is due to the small rate constant of the Fe^{2+} reaction with nitrous acid [10].

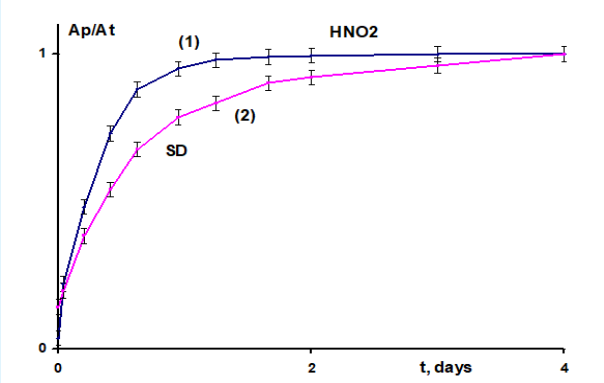

Figure 4: Dependence of relative absorbance Ap/At, where Ap – absorbance on the plateau, At – absorbance at give time t after treatment, days.

To estimate reaction time with the products formed under the action of pulse radiation of the spark discharge, a sample of Mohr's salt solution with a concentration of 20 g/L and a volume of 5 ml was treated with a spark discharge for three minutes. The choice of the concentration is related to the fact that the oxidation will not consume all of the ferrous iron. Immediately after treatment, the sample was diluted 100 times with 0.4 M sulfuric acid, since the absorbance in accordance with technical parameters of spectrophotometer should not exceed 2. The dependence of the ratio, Ap/At, from the time after processing is represented in Figure 4, curve 2. In that figure, the absorbance at 304 nm increases slowly and reaches a plateau four days after processing. This plateau can be explained both by the small reaction rate constant and by the formation of a complex under the action of radiation, which decays after 14 days. After four days, the concentration of complex decreases greatly [6], and the contribution to the total oxidation yield on the fourth day is within the measurements error. Therefore, in all experiments with Mohr's salt, the absorbance of the sample was measured for several days, and the yield of oxidizing equivalents was determined based on absorbance values at 304 nm collected on the fourth day after treatment. In all cases, when the absorbance at 304 nm reached the plateau, the ferrous iron remained in the solution, implying that there was no chain reaction.

Features of the Kinetics of Oxidative Reactions under the Action of Plasma Radiation

The Mechanism of Indirect Action of Radiation: When the sample was exposed to cold plasma, it reacted with all active species in the plasma itself. The concentration of active species in the plasma is constant, so the reactions under plasma began immediately after the plasma generator was turned on and continued at a rate determined by the composition of the sample and the concentration of active species.

However, when the sample is exposed to plasma radiation, it can directly absorption the photons as molecules of a substance dissolved in water; further chemical transformations were determined by the formation of secondary active species in the radiated water. If there are no chromophores directly absorbing radiation in the sample, the radiation itself does not have chemical activity. At the moment the radiation was turned on, active species in the sample are negligible, as they are just beginning to develop. Their concentration becomes substantial only after some time after the start of processing. Therefore, reactions under radiation are delayed.

To evaluate the role of the mechanism of action through secondary active species, experiments were performed for cases 1 and 2: exposure directly to the test substance dissolved in water (case 1) and pure water, to which the test substance was then introduced (case 2). Table 1 presents the results of the oxidation yield measurements, in which a solution of ferrous iron in the Mohr's salt was used as a test substance. The processing time in all modes was three minutes. In the processing modes of spark discharge generator SD50 "All" and "Gas" the oxidation yields for cases 1 and 2 are close in limit of measurement errors. This result means that the mechanism of indirect action of radiation through secondary active species is decisive. Table 1 also shows that the mechanism of indirect action takes place for processes under the action of continuous radiation from a UV lamp. This process also takes place for UV discharge plasma radiation when it affects the sample through quartz glass ("Quartz" mode). The yield of oxidants in the case of treatment through quartz glass is less than without the glass. This may be due to the attenuation of the photon flux by quartz glass at a wavelength of 200 – 250 nm (see Figure 2). The attenuation is 30% at 200 nm and 20% at 250 nm. The result indicates a large role of short-wave radiation. In addition, the decrease of the yield can be affected by the delay in production of the

active species under the radiation in the liquid after switching on the radiation source, which is discussed further in next section.

Mode of Treatment	Treated Sample	
	Mohr's Salt, case 1	Water, case 2
All	$(2.6 \pm 0.3) \times 10^{-2}$	$(2.3 \pm 0.3) \times 10^{-2}$
Gas	$(2.1 \pm 0.3) \times 10^{-2}$	$(2 \pm 0.3) \times 10^{-2}$
Quartz	$(2.4 \pm 0.6) \times 10^{-3}$	$(3.5 \pm 0.7) \times 10^{-3}$
UV lamp	$(1.5 \pm 0.4) \times 10^{-4}$	$(1.0 \pm 0.4) \times 10^{-5}$

Table 1: Yield of oxidation of the ferrous iron in Mohr's salt (mol equiv)/L for different treatment modes by the generator SD50 and UV mercury lamp. Sample volume was 5 ml and processing time for all samples was three minutes.

Table 1 shows that immediately after treatment, the concentration of oxidizing equivalents in water is $(2.3 \pm 0.3)\ 10^{-2}$ (mol equiv)/L. The product, which is directly identified by the absorption spectrum of the treated water sample, is nitrous acid [5]. The measured concentration of nitrous acid after treating the water sample for three minutes was $(2.35 \pm 0.25)\ 10^{-3}$ mol/L. The concentration of nitrous acid is small; therefore, only the formation of nitrous acid is impossible to explain the observed yield of the oxidizing equivalent. Hydrogen peroxide also cannot contribute because it interacts quickly with Fe^{2+} and as a result, the absorbance at 304 nm is small immediately after mixing the H_2O_2 and Mohr's salt solutions.

A large yield of ferrous iron oxidation could be associated with a chain reaction. Our experiments show that under the action of $HO_2^{\bullet}$, H_2O_2 and HNO_2, the chain reaction does not take place. If there were a chain reaction with the other unidentified oxidant, the ferrous iron would be consumed completely. However, less than 60% of ferrous iron is consumed during processing. In all cases, the oxidation reaction of ferrous iron stops, implying that the chain reaction with an unidentified oxidant does not take place. Therefore, when under the action of spark discharge some oxidants are formed in water, the concentration of these spark discharge oxidants are much higher than the concentration of oxidants that have been identified.

Table 2 compares the total number of oxidants formed in Petri dishes with different surfaces and different volumes of water in the "All" and "Gas" modes. Petri dishes of 5 and 50 ml volumes were used. A 5 ml dish with a diameter of 4 cm and a surface area of 12.5 cm^2 completely fell into the field of radiation. In a 50 ml dish with a diameter of 7 cm and a surface area of 38.5 cm^2, only a 4 cm diameter within the central region was irradiated. Table 2 shows that in the 5 ml dish in the "All" and "Gas" modes, the same amounts of oxidants are produced. In a 50 ml dish, the number of oxidants is 1.5 to two times greater than in 5 ml dish, even though the surface area and volume are three and 10 times larger, respectively. The "All" mode in a dish of 50 ml produces significantly more oxidants when compared to the "Gas" mode (see Table 2). This result means that the processes occurring in the field of radiation play the main role in the active species generation.

Mode	V = 5 mL	V = 50 mL
All	$(1.15 \pm 0.1) \times 10^{-4}$	$(2.16 \pm 0.15) \times 10^{-4}$
Gas	$(1.0 \pm 0.1) \times 10^{-4}$	$(1.52 \pm 0.15) \times 10^{-4}$

Table 2: Oxidants (mol equiv) produced in 5 and 50 ml water samples under action of the generator SD50 over three minutes.

Plasma radiation results in a complex production, which decomposing into $ONOOH/ONOO^-$, and generation of nitrous acid [6]. For nitrous acid, $pK_a = 3.4$. After three minutes of treatment, the acidity of the solution decreases to pH = 3.4 – 3.5. Under these conditions, nitrous acid exists in aqueous solution as NO_2^- ions with a probability of at least 50%. Therefore, the decay products of the complex will interact with NO_2^- ions [11]:

$$ONOOH + NO_2^- \leftrightarrow \text{adduct}^- \rightarrow NO_2^- + NO_3^- + H^+ \quad (5)$$

The rate of reaction 5 strongly depends on the concentration of reagents. The observed rate constant $k_{5obs} = 1.1 - 6\ s^{-1}$ [12]. Reaction 5 consumes peroxynitrous acid, and ions NO_2^-. This can stabilize the yield of oxidants in water after treatment in the "All" and "Gas" modes in a 5 ml dish. Therefore, the concentrations of oxidants (Table 1) and their contents in the sample (Table 2) after treatment in the "All" and "Gas" modes for the 5 ml dish are approximately the same.

In a 50 ml dish, the surface of the water is much larger. It is therefore logical that the amount of nitrogen oxides absorbed from the gas phase by water in 50 ml dish will be greater than in the 5 ml dish. However, the concentration of products formed in the water after absorption of nitrogen oxides in the 50 ml dish would be less than in the 5 ml dish, since the yield of nitrogen oxides formed in the discharge region does not depend on the sample surface. In both cases, this yield must remain the same and is determined by discharge characteristics.

Under radiation, more oxidants are formed, which do not terminate when interacting with other species in reaction 5.

Therefore, based on the data of Tables 1 and 2, the main reaction mechanism, initiated by spark discharge plasma radiation, is the indirect action of radiation through the formation of secondary active species, which firstly are produced and then interact with substances dissolved in water.

Delay in the Formation of Active Species: The dependence of the ferric iron concentration on processing time was studied to estimate the delay time of formation of active species after switching on the radiation source. The dependence of the concentration of oxidized ferric iron in the Mohr's salt (case 1, directly processed Mohr's salt), formed by the radiation of the generator SD50 during processing from one to five minutes in the "All" (curve 1) and "Gas" (curve 2) modes is presented in Figure 5. Similar dependences were obtained for case 2, when water is directly treated and subsequently mixed with Mohr's salt. The oxidation yields (Table 1) are close for these cases within the experimental error. The dependences can be approximated by straight line. Their continuation to the intersection with the time axis gives the value of processing time, after which the rate of oxidation reaction becomes noticeable. The reason for the delay in the beginning of the reaction may be because there is a lack of active species in the solution before the treatment, and the reaction rate constants for species formed under the radiation are small. In order for the reaction rate to become noticeable, the concentration of species must exceed the minimum value.

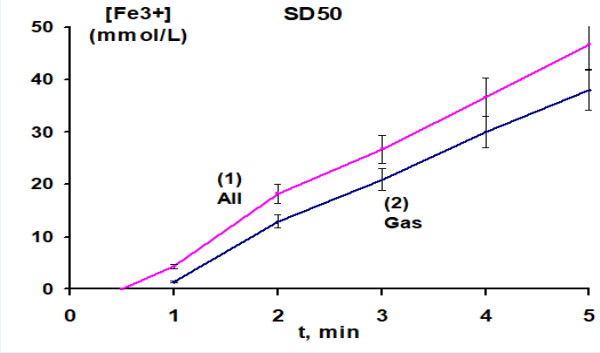

Figure 5: The dependence of the yield of oxidized ferric iron (mmol/L) in the sample of Mohr's salt solution, volume 5 ml, from the time of processing (minutes) by generator SD50 for modes: "All" – curve 1 and "Gas" – curve 2.

Figure 6 presents the dependence of concentration of ferric iron formed during the irradiation of samples by mercury UV lamp. In case 1, when the solution of Mohr's salt is processed directly, the reaction rate is constant, and the concentration of oxidized iron is linearly dependent on processing time (curve 1). In case 2, when water is irradiated and the Mohr's salt is subsequently introduced, the oxidation rate becomes noticeable for the treatment time after approximately one minute (Figure 6 curve 2). Under direct exposure to UV lamp radiation (case 1), the main active species are $HO_2^{\bullet}$ radicals [6], which interact rapidly with Fe^{2+}.

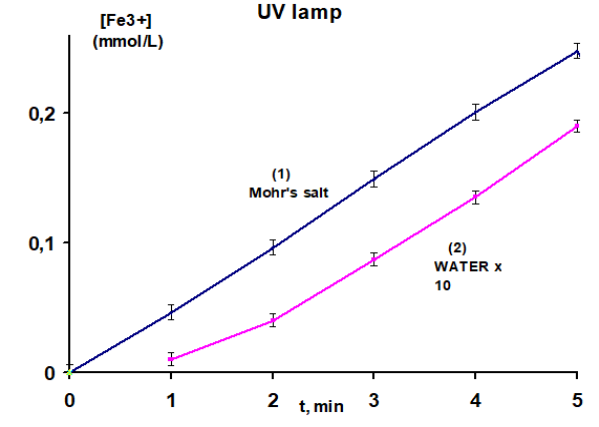

Figure 6: The time dependence of the yield ferric iron (mmol/L) in the Mohr's salt sample, curve 1, after processing by UV lamp (case 1) and in the water sample after processing by UV lamp radiation and the introduction of Mohr's salt (case 2), multiplied 10 times, curve 2.

For case 2, the secondary active species remaining in water after irradiation by UV lamp is hydrogen peroxide [8]. The reaction of the ferrous iron with hydrogen peroxide (Fenton reaction) is slow. Therefore, in order for the reaction rate to be noticeable, a certain amount of peroxide must be produced. Radicals $HO_2^{\bullet}$ can be quenched without the formation of peroxide. In addition, hydrogen peroxide decomposes under UV radiation. Therefore, the concentration of ferric iron in case 2 is much less than in case 1, yet the indirect effect radiation under the action of UV lamp radiation takes place. The oxidation for case 2 becomes noticeable after a processing time of at least one minute (Figure 6).

Both the radiation intensity of the mercury lamp used in this work and the radiation of the spark discharge

plasma were previously compared [13], reporting a yield of hydrogen peroxide decomposition and oxidation of the iodide ion in an aqueous solution under the condition of complete absorption of radiation in the sample of the detecting liquid. In that study, the intensity of the mercury lamp radiation is about 400 times greater than that of the spark discharge plasma radiation. This fact is not in doubt, since the power of the mercury lamp is 9 J/s with an efficiency of about 90% and the power released in the spark discharge of the generator SD50 is only 0.4 J/s. A much larger oxidation yield under plasma radiation at a considerably lower radiation intensity is associated with the reaction mechanism under pulsed radiation.

Reduction of Potassium Permanganate

Potassium permanganate in acidic media is an oxidant. The substance, which can interact with potassium permanganate, shows reductive properties. Therefore, the content of reducing agents was estimated using the test solution of potassium permanganate. The solution of 0.05N $KMnO_4$ was directly exposed to SD50 plasma radiation (case 1), and a solution of $KMnO_4$ was introduced into the sample of water treated with radiation (case 2). To measure the spectrum, all solutions were diluted 10 times after treatment. Then, the time required to complete the reduction reaction was determined. The reaction with nitrous acid was completed in two days; in both case 1 and 2, the reaction with a sample treated with plasma radiation was complete after four days. Absorbance lines ranging between 450 and 600 nm are observed in the initial potassium permanganate spectrum. When the manganese is reduced, the absorbance decreases; after full reduction of Mn^{7+}, the absorbance drops to zero and the solution becomes transparent and colourless.

An example of changes in the absorption spectrum of the $KMnO_4$ solution is presented in Figure 7. There was no visible appearance of other absorption lines between 400 and 600 nm, which would indicate the formation of intermediate products in the Mn^{7+} reduction. The $KMnO_4$ concentration was determined by the absorbance at 527 nm and the reducing equivalent yield was calculated by measuring the decrease in this absorbance value, considering that the normality of reaction was 5 (Mn^{7+} reduced to Mn^{2+}). The results are presented in Table 3. The table shows that for both oxidation and reduction processes, the mechanism of indirect action prevails. Almost the same yield of reducing equivalents in the "All" and "Gas" modes are associated, as well as in the case of oxidation, with the stabilization of their concentration due to the reaction 5. Measurements of time dependence of the reaction yield showed that there is a delay in the beginning of the reduction reaction for about one minute, as in the case of the oxidation reaction.

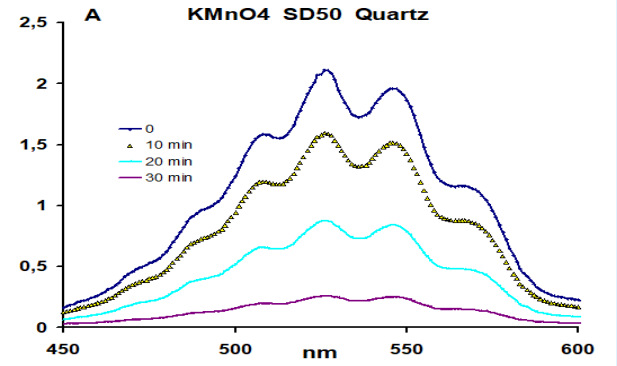

Figure 7: Change in absorption spectrum of $KMnO_4$ solution after treatment by radiation of generator SD50 through quartz glass.

Mode of Treatment	Treated Sample	
	Mohr's salt, case 1	Water, case 2
All	$(9.3 \pm 0.8)\ 10^{-3}$	$(8.3 \pm 0.6)\ 10^{-3}$
Gas	$(8.2 \pm 0.6)\ 10^{-3}$	$(8.1 \pm 0.6)\ 10^{-3}$
Quartz	$(4.1 \pm 0.4)\ 10^{-3}$	$(3.8 \pm 0.4)\ 10^{-3}$
UV lamp	$(4.4 \pm 0.5)\ 10^{-3}$	$(3.1 \pm 0.3)\ 10^{-3}$

Table 3: Yield of manganese reduction in potassium permanganate solution (mol equiv)/L, with a sample volume of 5 ml and treatment time 3 minutes.

Channels of Redox Reactions

The main products generated during sample processing by the generator of the spark discharge are: $HO_2^{\bullet}/O_2^{\bullet-}$ (pK_a=4.8), nitrous acid HNO_2/NO_2^- (pK_a = 3.4) and $ONOOH/ONOO^-$ (pK_a = 6.8); these products exhibit reductive and oxidative properties.

Reactions with Radical $HO_2^{\bullet}/O_2^{\bullet-}$: Radical $HO_2^{\bullet}/O_2^{\bullet-}$ (pK_a=4.8), species exist in an acidic medium as $HO_2^{\bullet}$ and exhibits oxidative properties. In a neutral or alkaline medium, however, this species exists in the form of the ion-radical $O_2^{\bullet-}$, which exhibits reducing properties. Water irradiated with generator SD50 after one minute of treatment has a pH < 4.8 (Fig. 3). The delay time of the beginning of the reaction is about one minute, so the radical $HO_2^{\bullet}/O_2^{\bullet-}$ in these experimental conditions can exhibit only oxidative properties. The interaction of ferrous iron in an acidic medium with $HO_2^{\bullet}$ radicals is described by the following reactions:

$$Fe^{2+} + HO_2^{\bullet} + H^+ \rightarrow Fe^{3+} + H_2O_2 \quad (6)$$

$k_6 = 1.5\ 10^6\ L(mol\ s)^{-1}$

$$Fe^{2+} + H_2O_2 \rightarrow Fe^{3+} + OH^{\bullet} + OH^- \quad (7)$$

$k_7 = 56\ L(mol\ s)^{-1}$

$$Fe^{2+} + OH^{\bullet} \rightarrow Fe^{3+} + OH^- \quad (8)$$

$k_8 = 10^9\ L(mol\ s)^{-1}$

$$HO_2^{\bullet} + HO_2^{\bullet} \rightarrow H_2O_2 + O_2 \quad (9)$$

$k_9 = 9.6\ 10^8\ L(mol\ s)^{-1}$

The data on the reaction rate constants from the Handbook [9] are used here. When considering reactions 6 – 9, one primary radical $HO_2^{\bullet}$ leads to oxidation of three ferrous iron ions. In this case we neglect the consumption of hydrogen peroxide under the action of UV-C radiation. However, the role of direct oxidation of ferrous iron by these radicals is small, since the concentration of oxidized ferric iron immediately after treatment is small (see Fig. 4).

Reactions with Nitrous Acid: Nitrous acid in our experimental conditions may exhibit both oxidizing and reducing properties. After three minutes of processing, the pH value does not exceed 3.3 and decreases with processing time (Fig. 3). Therefore, under our experimental conditions, nitrous acid equally exists in ionic and molecular form. The oxidation of ferrous iron by nitrous acid is as follows:

$$2HNO_2 + 2FeSO_4 + H_2SO_4 \rightarrow Fe_2(SO_4)_3 + 2H_2) + 2NO^{\bullet} \quad (10)$$

$$NO_2^- + Fe^{2+} \rightarrow Fe^{3+} + NO^{\bullet} + O^{\bullet} \quad (11)$$

The normality of the reaction used to determine the yield of oxidizing equivalents is 1. The reduction of manganese in acidic medium is as follows:

$$5HNO_2 + 2KMnO_4 + H_2SO_4 \rightarrow 2Mn(NO_3)_2 + K_2SO_4 + 3H_2O + HNO_3 \quad (12)$$

In equation 12, the oxidization of $Mn^{7+} \rightarrow Mn^{2+}$ required five electrons, nitrous acid, whereas the reducing agent $N^{3+} \rightarrow N^{5+}$ provided 2 electrons. The normality of the reaction used to determine the yield of the reducing equivalents is 5.

Reactions with Peroxynitrous Acid

The chemical $ONOOH/ONOO^-$ in an acidic medium is formed in the processing by generator SD50, exists in the form of peroxynitrous acid, as pH < pK_a. The properties of peroxynitrite and peroxynitrous acid were previously considered [14]. That study showed the oxidation reaction of Fe^{2+} with peroxynitrous acid in acidic medium to be:

$$Fe^{2+} + ONOOH + H^+ \rightarrow Fe^{3+} + NO_2^{\bullet} + H_2O \quad (13)$$

$$Fe^{2+} + NO_2^{\bullet} \rightarrow Fe^{3+} + NO_2^- \quad (14)$$

Two bivalent iron ions are oxidized by one molecule of peroxynitrous acid. The possible reaction of the manganese reduction in an acidic medium is as follows:

$$2KMnO_4 + 5ONOOH + 2H^+ \rightarrow 2MnO + 2KNO_3 + 2H_2O + 2O_2 + 3HNO_3 \quad (15)$$

The reactions of peroxynitrous acid with the test substances Fe^{2+} and $KMnO_4$ (equations 13-15) shows, that measured yield of oxidizing equivalents to be twice as great as the yield of reducing equivalents. This result may be one of the main reasons for the notably lower yield of reducing equivalents under the action of the SD50 generator when compared to the yield of experimentally observed oxidizing equivalents (see Tables 1 and 3). The chemical effect of plasma on aqueous solutions has been previously studied in detail [15]. The results obtained in our work complement these past data.

Conclusion

1. Under pulse plasma radiation, the mechanism of indirect action prevails, when the active species themselves are first formed in water. After formation, they can interact with substances dissolved in water.
2. When the radiation source is turned on, there are no active species in the liquid. The reaction begins after the concentration of active species reaches a significant level. Therefore, considering the specific conditions of the experiment there is a delay time of about one minute from the beginning of the reaction under radiation turn on.
3. Active species formed under the action of plasma radiation have both oxidizing and reducing properties.
4. The main contribution to the yield of redox reaction is complex, which directly unidentifiable; it decays into peroxynitrite and peroxynitrous acid.

References

1. Weltmann KD, Kolb JF, Holub M, Uhrlandt D, Simek M, et al. (2018) The future for plasma science and

technology. Plasma Processes and Polymers 16(1): 1-29.

2. Thirumdas R, Kothakota A, Annapure U, Siliveru K, Blundell R, et al. (2018) Plasma activated water (PAW): Chemistry, physico-chemical properties, applications in food and agriculture. Trends in Food Science & Technology 77: 21-31.

3. Piskarev IM (1998) Conditions of initiating reactions in liquid by gas phase active particles. Russian Journal of Physical Chemistry 72(11): 1793.

4. Piskarev IM (2016) Acid generating effect of plasma species and pulsed ultraviolet plasma radiation. High Energy Chemistry 50(4): 298-303.

5. Piskarev IM, Ivanova IP (2018) Effect of spark electric discharge between solid electrodes on water. Plasma Sources Sci Technol.

6. Piskarev IM, Astaf'eva KA, Ivanova IP (2017) The effect of pulse UV plasma irradiation of liquid through rat skin. Biophysics 62(4): 547-552.

7. Piskarev IM, Ivanova IP, Trofimova SV (2013) Chemical effects of self-sustained spark discharge: simulation of processes in a liquid. High Energy Chemistry 47(2): 62-66.

8. Piskarev IM (2018) Hydrogen peroxide formation in aqueous solutions under UV-C radiation. High Energy Chemistry 52(3): 212-216.

9. Haynes WM (2016-2017) Handbook of chemistry and physics. 97th(Edn.), CRC Press.

10. Epstein IR, Kustin K, Warshaw LJ (1980) A kinetic study of the oxidation of iron (II) by nitric acid. J Am Chem Soc 102(11): 3751-3758.

11. Piskarev IM (2016) Spark plasma radiation-induced formation of long-lived active species. High Energy Chemistry 50(5): 424-425.

12. Maurer P, Thomas CF, Kissner R, Riigger H, Greter O, et al. (2003) J. Phys. Chem. A 107: 1763.

13. Piskarev IM, Ivanova IP, Trofimova SV (2013) Comparison of chemical effects of UV radiation from spark discharge in air and low-pressure mercury lamp. High Energy Chemistry 47(5): 247-250.

14. Lobachev VL, Rudakov ES (2006) The chemistry of peroxynitrite. Russian Chemical Reviews 75(5): 422.

15. Brisset JL, Pawlat J (2015) Chemical effects of air plasma species on aqueous solutes in direct and delayed exposure mode: discharge, post-discharge and plasma activated water. Plasma Chem Plasma Process 36(2): 355-381.